Supplementary Information:

Photomechanical Structures Based on Porous Alumina Templates Filled with 9-Methylanthracene Nanowires

Adam J. Berges[1], Wangxiang Li[1], Wenwen Xu[2], Fei Tong[1,a], Rabih O. Al-Kaysi[3], Ryan C. Hayward[2], Christopher J. Bardeen[1]*

[(1)] Department of Chemistry
University of California, Riverside
Riverside, CA 92521 (USA)

[(2)] Department of Chemical and Biological Engineering
3415 Colorado Ave.
University of Colorado Boulder
Boulder, CO 80303

[(3)] College of Science and Health Professions-3124,
King Saud bin Abdulaziz University for Health Sciences, and King Abdullah International Medical Research Center, Ministry of National Guard Health Affairs, Riyadh 11426,
Kingdom of Saudi Arabia

* corresponding author: christopher.bardeen@ucr.edu; ORCID: 0000-0002-5755-9476

[a] current address:
School of Chemistry and Molecular Engineering
East China University of Science and Technology
Shanghai 200237
The People's Republic of China

Table of Contents

1. Solvent annealing apparatus and nanowire preparation

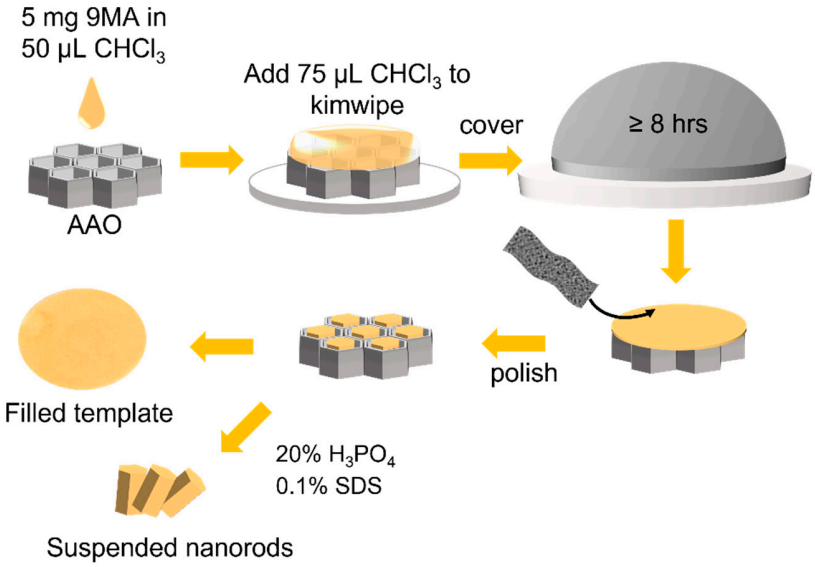

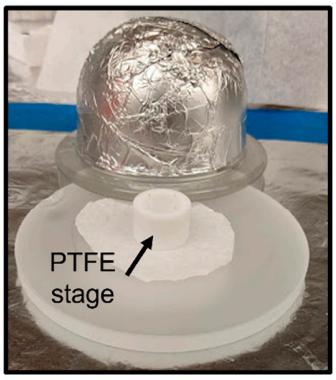

Figure S1 Flowchart detailing the new template filling procedure for **9MA** in chloroform. Templates are pre-washed in chloroform before solution is added to the surface. Once dry, each sample is polished with 9 µm Al2O3, 5 µm SiC, 2 µm, 1 µm, 0.3 µm Al2O3 lapping paper. Inset: photograph of the apparatus used.

In order to fill templates using the procedure from the text, empty AAO templates are placed on the Teflon stages after initial wetting in pure $CHCl_3$. The volume of $CHCl_3$ added to the Kimwipe below the stage depends on the volume of the bell jar used. Typically, enough solvent is used to saturate 110% of the volume of the bell jar (e.g. for a 163 cm^3 bell jar, a total volume of 125 µL is used, corresponding to a ≈ 180 cm^3 container). Each bell jar is covered with aluminum foil in order to prevent photodimerization of the **9MA** during the annealing process. Figure S1 describes the processing of the AAO templates with the apparatus included as an inset.

2. Density of AAO templates

The skeletal density of the AAO templates is determined using Archimedes principle to measure the weight of individual templates first in air and then in ethanol to mitigate formation of air bubbles on the surface of the sample. Samples are measured in a mesh weigh boat suspended from the eyelet on the bottom face of the scale (AND HR120 analytical balance) so that the samples can be submerged in the auxiliary liquid. The temperature of the auxiliary liquid is monitored with a k-type thermocouple. The apparent weights are used in the following equation to determine the density of the sample ρ_i:

$$\rho_i = \frac{W_{air}}{W_{air} - W_{EtOH}}(\rho_{air} - \rho_{EtOH}) + \rho_{EtOH}$$

where W_{air} is the weight in air, W_{EtOH} is the weight in ethanol, ρ_{air} and ρ_{EtOH} are the densities of air and ethanol respectively. The skeletal density is averaged across 10 different AAO templates and a cartoon of the set-up is included below in figure S2.

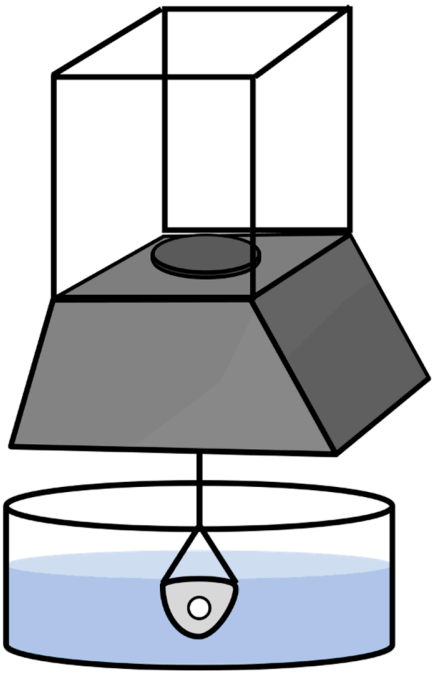

Figure S2 Cartoon of the apparatus used to measure the skeletal density of the AAO templates. Individual templates are supported in a mesh weigh boat and first measured in air, then completely submerged in the auxiliary liquid.

From the skeletal density (ρ_{skele}) of the AAO, we can determine the effective porosity of the templates. Given that a 60 µm thick, 13 mm diameter disk solid disk (V_{disk}) would have a volume of ≈ 7.96 * 10^{-2} cm^3, then it should have a weight of $W_{disk} = \rho_{skele} * V_{disk} \approx 23.9$ mg. Using the average observed weight of the porous template, $W_{AAO} = 10.0 \pm 0.1$ mg, then the volume of the void space and the porosity (P) of the template can be calculated using:

$$V_{void} = \frac{W_{disk} - W_{AAO}}{\rho_{skele}}$$

$$P = \frac{V_{void}}{V_{disk}} = \frac{W_{disk} - W_{AAO}}{W_{disk}} = 1 - \left(\frac{W_{AAO}}{W_{disk}}\right)$$

Using the above equations, the porosity of the templates used is approximately 58 ± 0.6 % and corresponds to ≈ 4.7 mg of 9MA as the weight of theoretical maximum fill.

3. Contact angle measurements of surface-functionalized templates

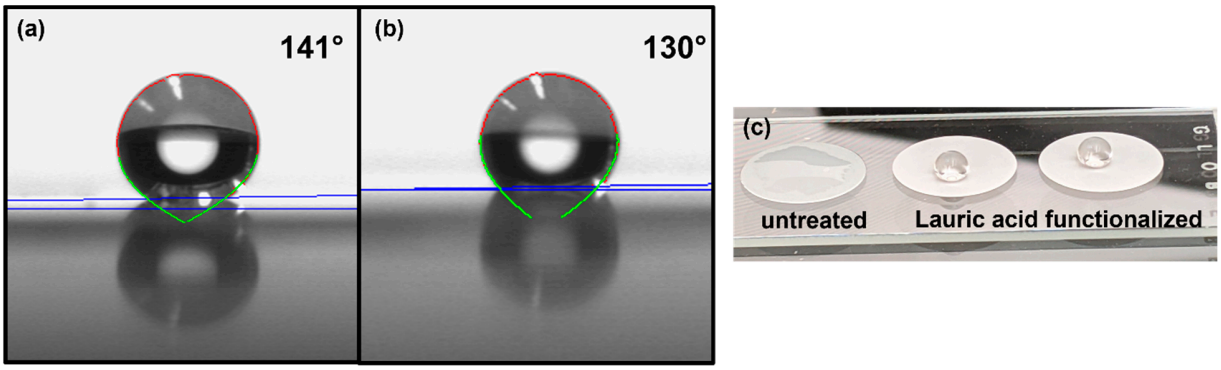

Figure S3 (a-b) Contact angle measurements of a 50 µL water droplet on a LA-functionalized AAO surface. Samples demonstrate superhydrophobic surfaces with contact angles ≥ 130°. The untreated AAO templates are sufficiently hydrophilic to form contact angles below the limit of detection of the instrumentation. Side by side qualitative comparisons are captured in **(c)** using 100 µL of water added to each surface via micropipette.

4. Comparison of surface functionalized templates

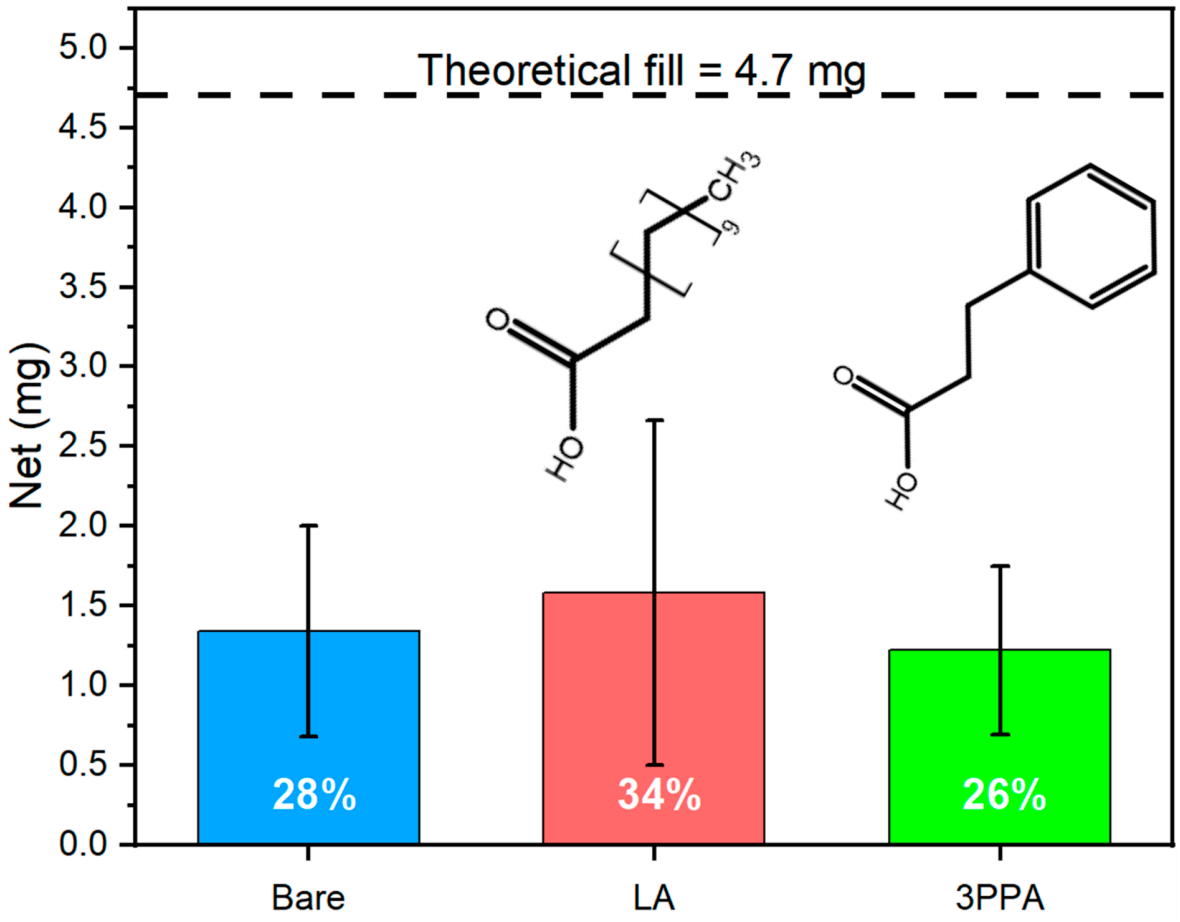

Figure S4 Comparison of the effect of surface functionalization on the AAO templates using the excess solvent method. Compared to the bare template, functionalizing the surface with lauric acid (LA) or 3-phenyl propanoic acid (3PPA) had a negligible effect outside of the margin of error.

Templates functionalized with lauric acid (LA) and 3-phenylpropanoic acid (3PPA) had no discernible impact on the net loading of the templates outside the margin of error. Each sample was prepared using the excess solvent method and produced similar results regardless of the functionalization reagent. The critical step in the solvent annealing process is saturating the solvent vapor in the annealing chamber, although the theoretical maximum loading still cannot be achieved.

5. Reaction progress as a function of exposure duration

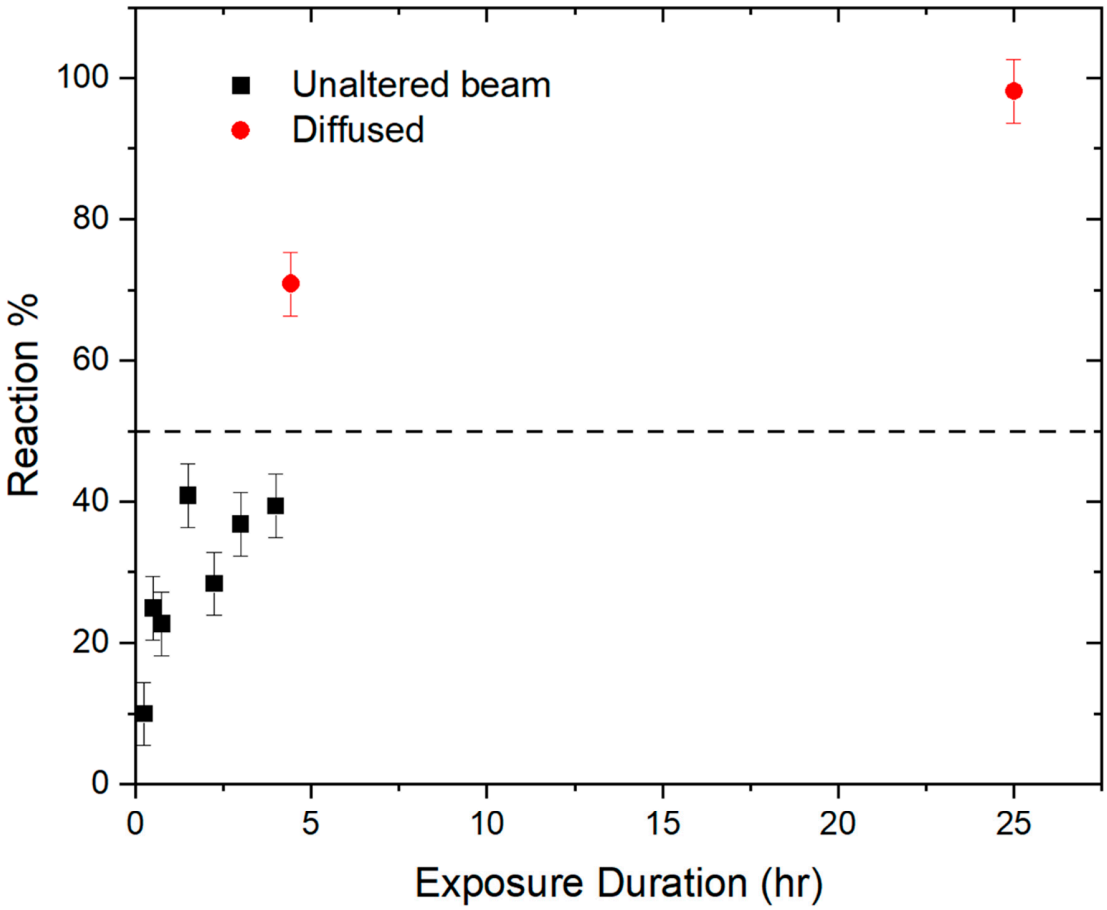

Figure S5 The percentage of the template that has been reacted when exposed to different durations of the UV source. In the first series, the beam spot size was approx. 96 mm^2 with a power density of ≈ 18 $\mu W/mm^2$. In the second series, the beam was expanded with a diffuser to complete cover the template at the sample stage with a power density of ≈ 19.5 $\mu W/mm^2$.

Samples are first irradiated in the interferometer apparatus and then dissolved in $CHCl_3$, then afterwards the absorbance of the solutions and promptly measured at room temperature in a 1 cm beam path cuvette. The concentration of the remaining **9MA** calculated from the Beer-Lambert law and converted into a total mass of remaining **9MA** (W_{rxn}) before comparing to the original net loading in the template (W_0). The reaction progress is thus W_{rxn} / W_0. In the first series, the 405 nm laser is unaltered and ≈ 96 mm^2 of the template is irradiated, depicting an asymptotic approach toward 50% completion. If the beam is diffused with an optical diffuser, exposing the entire sample stage, then the reaction can proceed to nearly 100% over the course of 25 hrs.

6. Model for fitting a coupled angular & linear displacement Michelson Interferometer

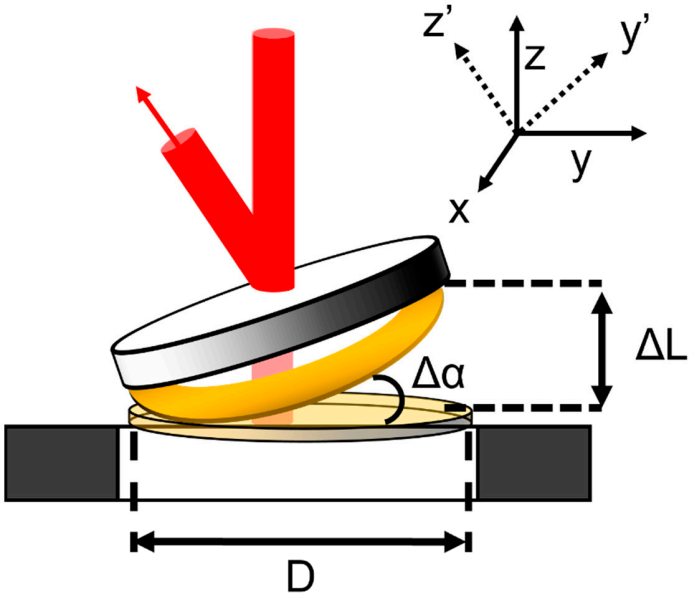

Figure S6 Cartoon of the Michelson interferometer at the sample beam path. When the template deforms and tilts the mirror, the angular displacement (Δα) and optical beam path difference (ΔL) can be coupled geometrically. This causes the sample beam path to tilt in the yz-plane, giving rise to the $E_2(x',y',z')$ field.

The misalignment of a two-beam interferometer can be described as the intensity change in the sum of the two electric fields $E_1(x,y,z)$ and $E_2(x',y',z')$, where E_1 is the field from reference path and E_2 is the field from the misaligned sample path. Assuming an infinite confocal parameter and radius of curvature while neglecting the Guoy phase shift, then the beam waist is also unchanged. If we consider only the misalignment in the yz-plane with the tilt angle α resulting in an optical beam path difference L, then the fields can be described as:

$$E_1(x,y,z)=A\cdot\exp\left(-\frac{(x^2+y^2)}{w^2}\right)\cdot\exp(kz-\omega t)$$

$$E_2(x',y',z')=A\cdot\exp\left(-\frac{\left(x'^2+y'^2\right)}{w^2}\right)\cdot\exp(kz'-\omega t)$$

where k is the wavevector of the laser source and A is the amplitude. If the angular tilt is assumed to be small, then $\sin(\alpha)\approx\alpha$, then the transformation of $(x,y,z)\rightarrow(x',y',z')$ can be simplified to:

$$x'=x$$
$$y'=y-(z-L)\alpha$$
$$z'=z-L+y\alpha$$

After taking the sum of E_1+E_2 and simplifying, the intensity of the two combined beams is:

$$I=\iint |E_1+E_2|^2 dxdy$$

$$I=\iint I_0\left(1+\exp\left(-ik(y\alpha-L)-\frac{-2y(z-L)\alpha+(z-L)^2\alpha^2}{w^2}\right)\right)dxdy$$

$$\text{where } I_0 = A\cdot\exp\left(i\omega t-\frac{x^2+y^2}{w^2}-ikz\right)$$

which resolves to eqn 2. in the main text. If the optical beam path difference is coupled to the angular offset, then the change in L is:

$$\Delta L=\frac{D}{2}\sin(\Delta\alpha)\approx\left(\frac{D\times\Delta\alpha}{2}\right)$$

where D is the diameter of the template.

7. Examples of interferogram variance

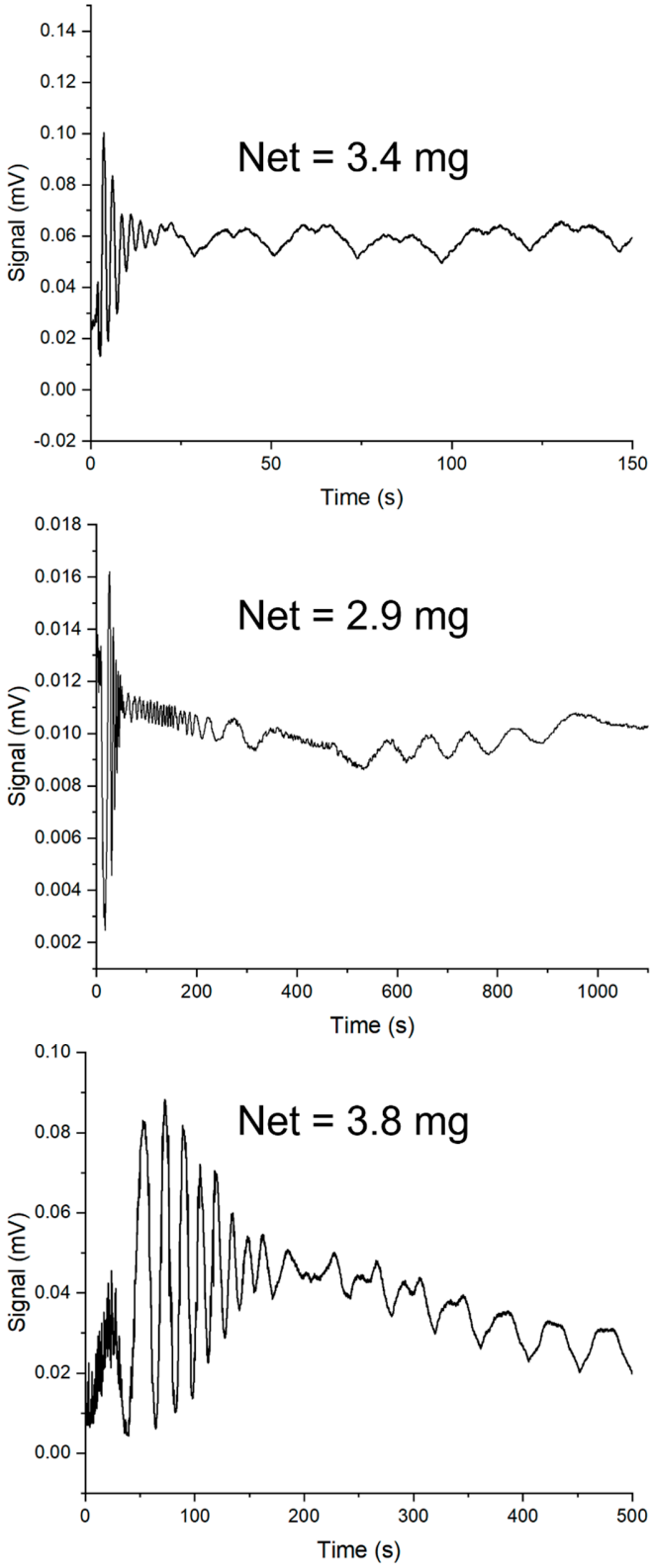

Figure S7 Example interferograms collected from three different templates filled with 9MA. The dominant behavior of each interferogram is the angular off-set building during the exposure duration, leading to the damping of the fringe heights. This angular error appears to vary significantly from sample to sample.